Int. J. Electrochem. Sci., 13 **(2018)** 11480 – 11490, doi: 10.20964/2018.12.69

International Journal of
ELECTROCHEMICAL
SCIENCE
www.electrochemsci.org

Preparation of Nitrogen Doped Lignin derived Porous Carbon for Supercapacitors

Tianyao Jiang[1], *Qingyang Sun*[1], *Wenbiao Xu*[2], *Guangzhen Zhao*[1], *Junyou Shi*[1,3,*]

[1] College of Chemical Engineering, Northeastern Electric Power University, China
[2] College of materials science and engineering , Northeast Forestry University, China
[3] Forestry College, Beihua University, Jilin 132013, China
[*]E-mail: bhsjy64@163.com

Received: 4 September 2018 / *Accepted:* 29 September 2018 / *Published:* 5 November 2018

We show the use of lignin as a carbon source to prepare electrode materials using nitrogen-doped, nitrogen doping introduces a nitrogen functional group to increase the hydrophilicity and active sites of the electrode material. Due to its high specific surface area (870.2 m^2 g^{-1}) and porosity, the introduction of functional groups can increase the charge transfer rate, Ultimately, the electrode has a high specific capacitance (320.4 F g^{-1} at a current density of 0.5 A g^{-1}), excellent rate performance and cycle stability (94.1% specific capacitance retention after 5000 cycles). The results of the above studies indicate that a low-cost, high-performance supercapacitor can be fabricated using abundant waste lignin.

Keywords: Nitrogen-doped, high specific surface, active sites

1. INTRODUCTION

Nowadays, fossil energy is rapidly decreasing and the environment is deteriorating [1]. The energy storage devices manufactured by people can reduce the consumption of natural energy and improve the utilization rate of waste materials [2], it is gradually moving towards a green, sustainable direction [3,4]. Supercapacitors are used in automotive, electronic, mobile power supplies, etc. They are divided into electrochemical double-layer capacitors and tantalum capacitors. Compared with other types of batteries, it has high energy density [5], long (and stable) cycle life, and low maintenance cost, which has attracted wide attention from scholars. Carbon materials are the more commonly used electrode materials [6,7], with many types, high specific surface area and good electrical conductivity [8,9], however, the lower specific capacitance and complicated synthetic route limit the application of carbon materials. Therefore, we need to explore a simple and economical method for preparing electrode materials [10].

There are many kinds of biomass in nature, the materials of carbon sources are different [11], and the electrochemical properties are slightly different. Many scholars today use aloe, rice husks, fungus, and stems of plants as carbon sources [12,13], They are used in a variety of activation methods, and some scholars have added N-based elements to increase electrochemical performance [14,15]. Lignin is the third largest natural organic matter in nature [16,17]. It has a large annual output and is primarily used in the pulp and paper industry. Today's scientific research technology is limited, and it is not fully utilized for lignin, and it is mostly waste [18]. Most of the lignin constituent elements are carbon elements [19,20], which are activated by high temperature (with inert gas protection) to raise the specific surface area and mesoporous ratio of carbon [21]. The closer the pore size of the carbon is to the size of the ions in the electrolyte [22], the higher the charge transfer rate, and the resulting porous carbon has good electrical conductivity. Many scholars have found that the doping of nitrogen functional groups on the basis of carbon materials is beneficial to the hydrophilicity of carbon materials [23-26], increasing the effective active sites of ion transport in electrolytes, achieving fast and efficient charge transfer rates, ultimately improve the electrochemical performance of supercapacitors [28].

In this paper, a simple preparation method is used to manufacture supercapacitors. Using cheap and abundant lignin as a carbon source, F127 as a template, and doping with a nitrogen-containing organic salt [15,29], the carbon material is obtained to obtain a nitrogen-containing element (3.39%) and a large specific surface area, improving the conductivity of the electrode and reduce its impedance.

2. MATERIAL AND METHODS

2.1 Synthetic nitrogen-doped porous carbon

The solid lignin (99% purity) is mixed with the templating agent (Pluronic F127) in a mass ratio, and more tetrahydrofuran (THF) and a small amount of hydrochloric acid (6 M) are added, after mixing, it was stirred at room temperature for 11 hours, added with nitrogen-containing organic salt (tetrasodium salt of ethylenediamine tetraacetic acid) and stirred for 24 h, and taken out into a tray, dry under vacuum at 70 ℃ for 24 h, carbonize under N_2 (appropriate flow rate) protection at 800 ℃ for 0.5~2 hours (Corresponding to No. 1~4).

2.2 Characterization methods

The morphology and particle size of the material is studied by field emission scanning electron microscopy (SEM, SU70-HSD) and higher resolution transition electron microscope (TEM, JEOL JEM2010). The crystallinity of the powder was recorded by X-ray diffraction (XD-2X/M4600, Cu Kα λ=1.54051 Å). Raman spectra were conducted on a LabRAM HR800 Raman spectrometer. The surface elemental composition was measured by X-ray photoelectron spectroscopy (Elmer PHI 550 spectrometer). The size distribution and specific surface area of the pore is collected respectively by using the BET equation and Barret-Joyner-Halenda (BJH) model.

2.3 Electrochemical measurement

The electrochemical measurements were carried out in three electrode on a CHI 760D electrochemical workstation, which equipped with a reference electrode (Ag/Agcl), a counter electrode (platinum gauze) and a working electrode just the nitrogen doped carbon electrode. Material was measured using cyclic voltammetry (CV), galvanostatic charge–discharge (GCD) and electrochemical impedance spectroscopy (EIS). Measurements were conducted in an aqueous electrolyte solution (6 M KOH) at 25 ℃. The mixture of active material, carbon black and polytetrafluoroethylene (PTFE) binder with a mass ratio of 8:1:1 was coated onto the nickel current collector (with a size of around 1 cm ×1 cm). The electrode coated with abovementioned fabricated paste (Approximately 2 mg) was dried overnight at 75 ℃. The specific capacitance (C_g, $F\ g^{-1}$) was calculated based on the formula of $C_g = (I*\triangle t)/(m*V)$, where I(A) is discharge current, $\triangle t$(s) is the discharge time, V(V) is the potential window during discharge and m(g) is the mass of active material on electrode.

3. RESULTS AND DISCUSSION

3.1 Microstructure characterizations

In order to investigate the microscopic crystal structure of the material, XRD is used to characterize it as shown in Fig. 1a, it is very clear that the graphite peak is at 23 (002) degrees. This can be observed that the nitrogen-doped carbon material is moderately crystalline, however No. 3 moved slightly to the right and had the best crystallinity. The Raman spectrum is shown in Fig. 1b, the two main peaks indicate the degree of graphite and non-graphitization of the sample, the G (1590 cm^{-1}) band is derived from bond stretching of sp2 carbon pairs in both rings and chains, D (1350 cm^{-1}) band originates from the breathing mode of aromatic ring, the ratio of the two is used to characterize the degree of crystallization. The results of the two characterization methods are consistent.

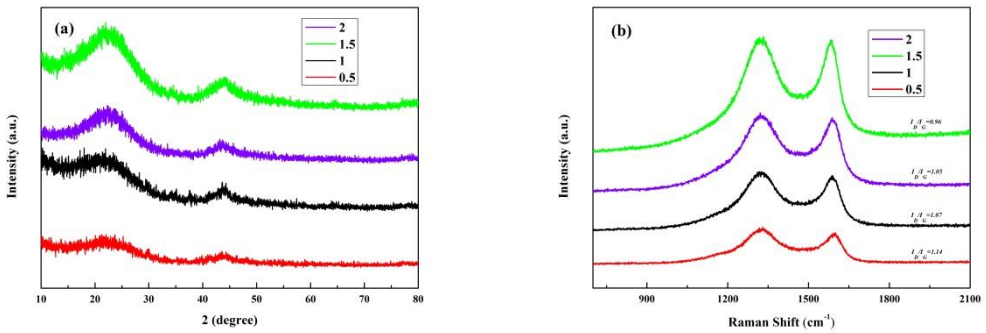

Figure 1. (a) XRD patterns and (b) Raman spectra of No1~4, respectively.

Studying the pore size distribution and specific surface area of nitrogen-doped carbon materials, using nitrogen adsorption isotherms, as shown in Fig. 2, indicating the existence of micropores and mesopores, most of the pores have a diameter of about 30 nm, microscopic apertures demonstrated by

SEM and TEM (Fig. 3a~f), it shows a certain degree of ordered honeycomb coal structure (The picture shows that it is more orderly than the carbon Xu Bin made [5]). Along with rising activation time from 0.5 h to 2 h, specific surface areas reached 384.1, 553.9, 663.7 and 737.5 m^2 g^{-1} (Table.1), the specific surface area of the material increases as the carbonization time increases. No.4 exhibits a high BET specific surface area of 737.5 m^2 g^{-1}, and the micropore volume reaches 0.09 cm^3 g^{-1}, it accounts for 29% of the total pore volume. The specific surface area of the sample is significant for electrochemical performance, but it is not a determining factor.

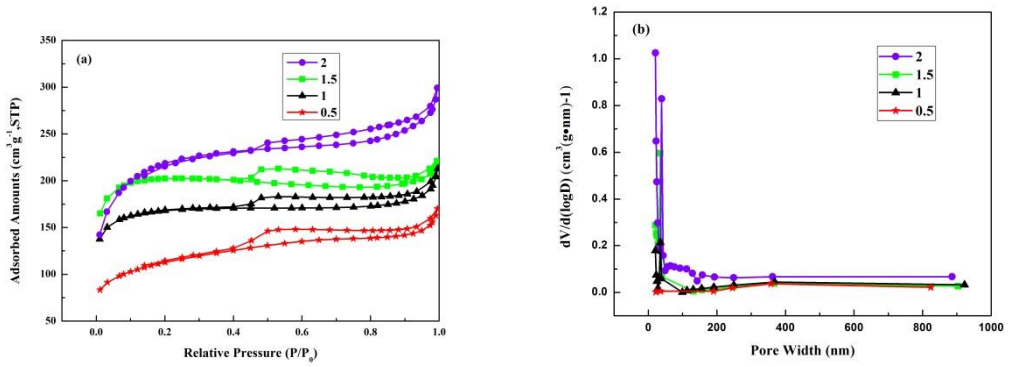

Figure 2. (a) BET nitrogen adsorption–desorption isotherm and (b) Corresponding pore size of No1~4, respectively.

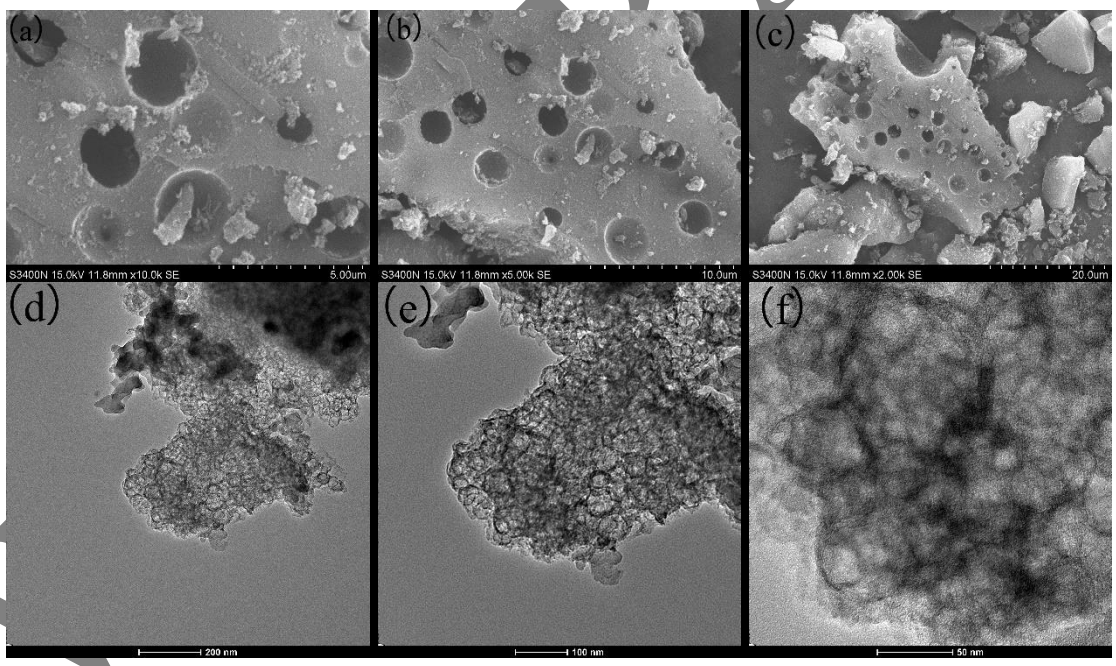

Figure 3. SEM (a~c) and TEM (d~f) image of No.3.

The closer the pore size of the material is to the size of the conductive ions, the smaller the internal resistance, this hierarchical porous structure with high surface area plays a key role in enhancing ion transport and charge storage.

Table 1. Physical properties including the surface area, pore volume and size.

Sample	S_{BET} (m^2 g^{-1})	S_{micro} (m^2 g^{-1})	V_{micro} (cm^3 g^{-1})
1	384.1	170.2	0.08
2	553.9	436.9	0.21
3	663.6	569.1	0.27
4	737.5	214.7	0.09

XPS measurement spectrum (Fig. 4) measured the existence of O and N functional groups in carbon atom, the existence of functional groups can not only improve the hydrophilicity of materials, but also provide additional pseudopotential for raw materials [33]. The increase of carbonization time will increase the content of O and N functional groups, however the nitrogen and oxygen hybridization is unstable under high temperature conditions and the content of O and N functional groups will decrease when the time is too long [34].

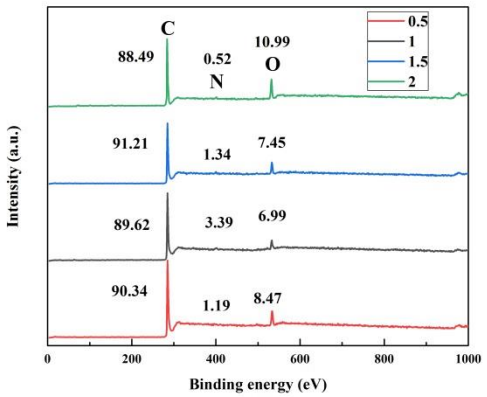

Figure 4. The XPS survey spectra of the samples.

Table 2 shows the range of changes of the N, O, and c elements. The N1s spectra indicate the residual nitrogen atoms in the carbon network were within four different environments: pyridinic (N-6, 398.7), pyrrolic/pyridone (N-5, 400.3 eV), quaternary (N-Q, 401.4 eV), and pyridine-N-oxide (N-4, 403 eV). The change of N-6 and N-5 content at the edge of carbon is illustrated, can represent the pseudo-capacitance effect (Fig. 5) [32-35], due to the lone pair of a nitrogen atom. Good performance corresponds to high content, N-6 percentage increased from 23.5% to 69.2%[15], whereas N-5 percentage decreased from 4.3% to 24.9% in No.1~4, The No. 3 material has the highest content of N-5 and N-6, which not only improves the hydrophilicity of the material, but also provides more effective active sites. Multiple C chemical states on the surface of carbons were confirmed by high resolution of C1s peak (Fig. 6), which can be deconvoluted into peaks at around 284.5, 285.1 and 287.4 eV, corresponding to C–C/C=C, C–O/C=N and C=O/C–N, respectively, No. 3 and No. 4 correspond to higher C–O/C=N and C=O/C–N contents. For comparison, the quantitative analysis results of the products prepared at different pyrolysis times are listed in Table 2, the carbon source is lignin, and it is

hard to achieve carbon with high porosity and high nitrogen content. After pyrolysis for 0.5 to 1.5 hours, the N content increases, while the 2-hour N content decreases.

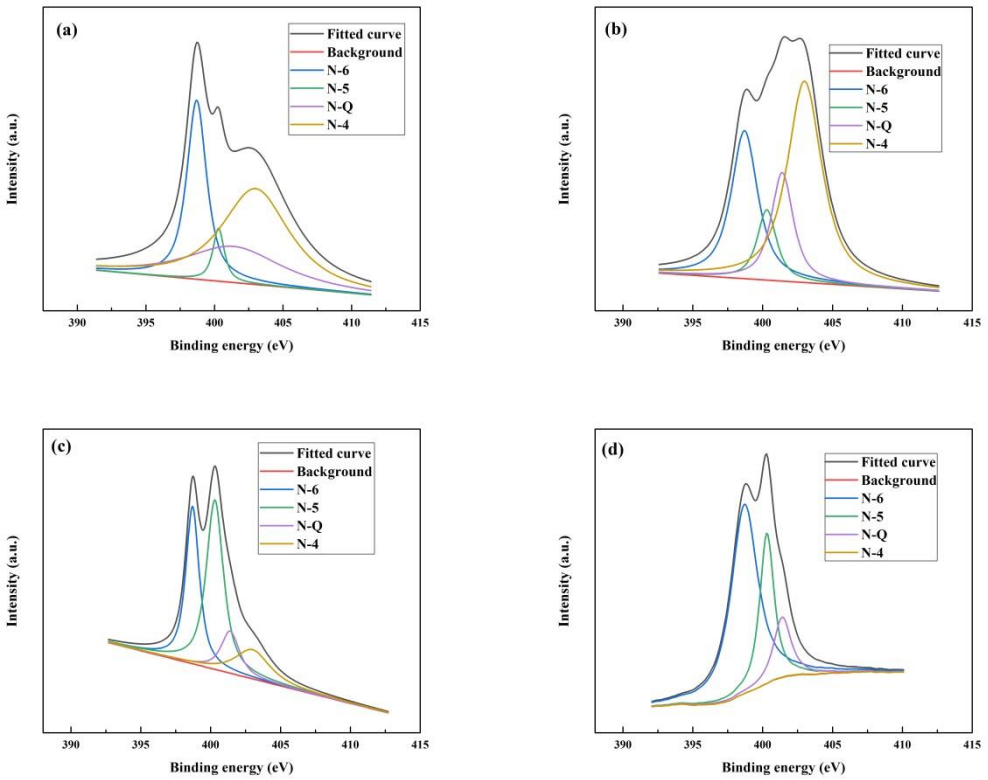

Figure 5. High-resolution N1s XPS spectra (a) No.1, (b) No.2, (c) No.3 and (d) No.4.

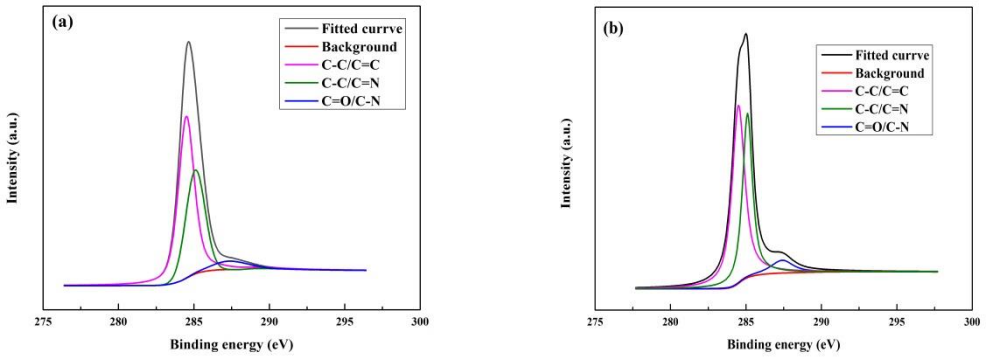

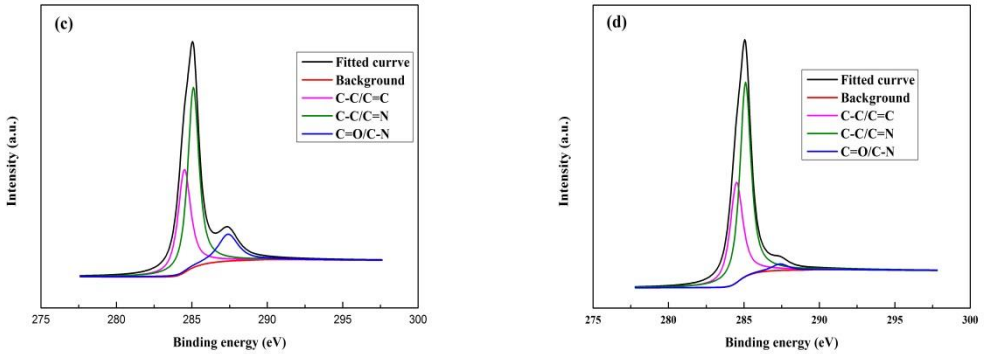

Figure 6. High-resolution C1s XPS spectra (a) No.1, (b) No.2, (c) No.3 and (d) No.4.

Table 2. Percentage of various species of nitrogen (and carbon) in the total nitrogen (and carbon) of the samples.

Sample	C–C/C=C	C–O/C=N	C=O/C–N	N-6	N-5	N-Q	N-4
1	54.4	38.8	6.8	25.3	4.3	24.6	45.8
2	58.3	36.3	5.4	23.5	9.8	17.3	49.4
3	34.1	51.7	14.2	46.8	24.9	12.6	15.7
4	36.3	60.6	3.1	69.2	19.2	9.5	2.1

3.2 Electrochemical behaviors

We investigated the electrochemical performance of N-doped porous materials, it was measured by galvanostatic charge/discharge (GCD) (at a current density of 1 A g^{-1}) and cyclic voltammetry (CV), in the symmetrical three-electrode system, the electrolyte was 6 $molL^{-1}$ KOH aqueous, it has a curve that approximates the shape of a rectangle, demonstrating the slight pseudocapacitance. In comparison with the CV curves of No.1~4, the curve of No.3 exhibited a larger rectangular sharply (Fig. 7a), it demonstrates the excellent electrochemical performance, this result can be attributed to the difference in pore size distribution and the introduction of nitrogen functional groups. Fig. 7c illustrates the CV curves of No.3 at different scan rates from 10 to 400 m Vs^{-1}. To investigate the electrochemical stability of the materials, the GCD cycling of No.1~4 was performed at a current density of 1 A g^{-1} (Fig. 7b) (Galvanostatic charge/discharge time is longer than 220s [5]or 235s [29]), Fig. 7d presents the GCD curves of No.3 at various current densities from 0.5 A g^{-1} to 10 A g^{-1}. The pore size of the material is mostly distributed at 40nm, which promotes the rapid transfer of ions in the electrolyte, however, the main reason is due to the doping of N, O functional groups [33]. The shape of the curve is symmetrical triangle with slight deformation, which is attributed to the influence of pseudo capacitance and double-layer capacitance.

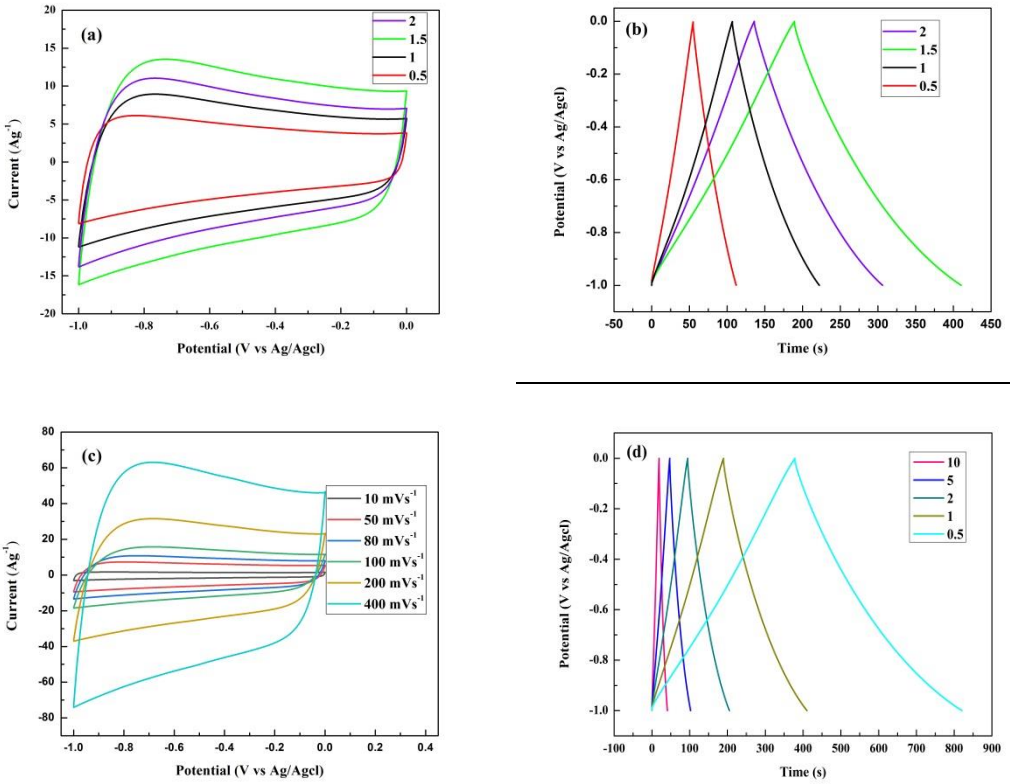

Figure 7. (a) CV curves at 100 mV s^{-1}, (b) GCD curves at 1 A g^{-1}, (c) CV curves of No.3 capacitor at various scan rates, (d) GCD curves of No.3 capacitor at various current densities.

The Nyquest plots (Fig. 8) shows a line near 72 degrees in the low frequency area, the radius of the semicircle indicates the charge transfer resistance, the material has the lowest impedance when the carbonization time is 1.5 hours. Low ion transfer impedance is attributed to pore size distribution and nitrogen doping, it can increase the hydrophilicity of materials, provide more effective active sites, and reduce charge transfer impedance. Ion transfer rate is very important in electrode materials of supercapacitors.

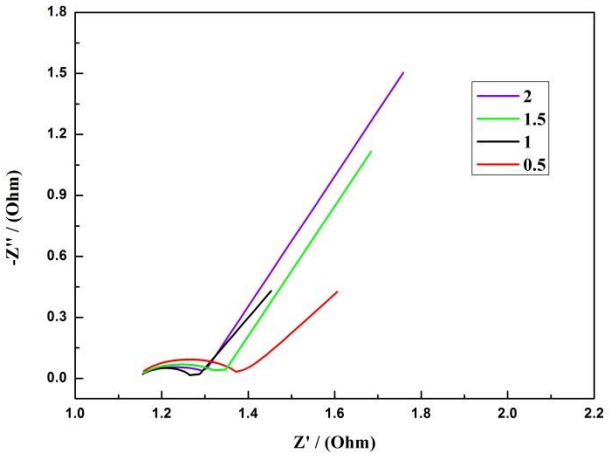

Figure 8. Nyquist plots of four sample capacitors.

Cyclic durability is an important index for measuring electrode materials (When the current density is 0.5 A g^{-1}, the specific capacitance is 201.2 F g^{-1}). It is measured in the two electrode system. When the current density is 10 A g^{-1}(Fig. 9), after 5000 cycles of test, the specific capacitance can still reach 89.5% (As shown in Table 3, compare the properties of several materials). No. 3 has no obvious attenuation, indicating that it has excellent stability, the high N content and uniform distribution of pore structure result in low mass mass transfer resistance. All those prove that Nitrogen doped carbon is very stable with cycling.

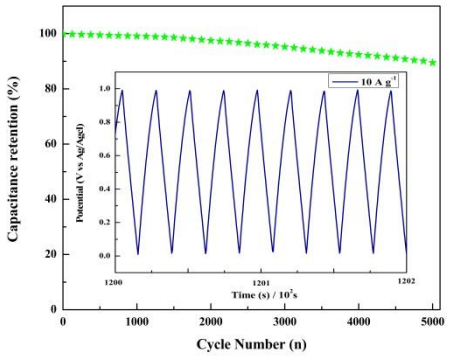

Figure 9. The cycling performance of No.3 capacitor at 10 A g^{-1}.

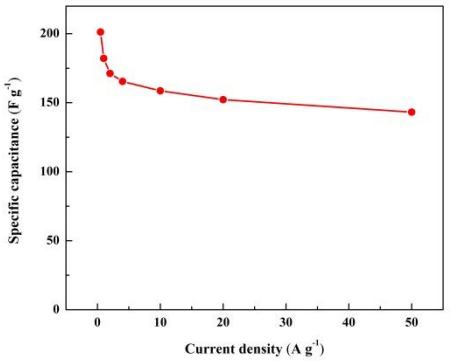

Figure 10. Specific capacitances of No.3 electrode based on galvanostatic charge/discharge curves from 1 to 50 A g^{-1}.

Table 3. Comparison of cycle stability, specific surface area and specific capacitance of different materials

Carbon source	S_{BET}(m^2 g^{-1})	Cyclic stability (%) (5000 times)	Specific capacitance(F g-1)	Electrolyte	Ref
Rice husk	1225	88 (2000 times)	115	1M H_2SO_4	12
Lignin	712	93.4	186.3	1M H_2SO_4	26
Lignin	1148		102.3	6 M KOH	36
Bamboo carbon	1732	84	222	6 M KOH	37

papaya	2664	98.7 (3500 times)	98.47	1M Na_2SO_4	38
Lignin nanofiber		83 (1500 times)	205	0.5M Na_2SO_4	39
N-doped carbon	267	70 (1000 times)	146	6 M KOH	40

4. CONCLUSIONS

Sample has good electrochemical properties and is attributed to its unique characteristics. Firstly, the templating agent F127 can make the arrangement of the holes more orderly. Secondly, high specific surface area and high void ratio of the material, providing sufficient space for charge transfer. Finally, the doping of nitrogen can increase the effective active site and hydrophilicity of the material, shorten the ion transport distance and polarization effect, which can increase the electron transfer rate and add extra capacitance. Electrode materials with the above advantages have excellent cycle stability. The results show that materials made from waste biomass can be used on supercapacitors.

References

1. L.L. Jiang, L.Z. Sheng, X. Chen, T. Wei, Z.J. Fan, *J. Mater. Chem.*,4 (2016) 11388.
2. H. Zhang, *Acs Nano*, 9 (2015) 9451.
3. S. Yan, J.J. Lin, P. Liu, S. Han, *RSC Adv*., 8 (2018) 6806.
4. D.P. Saha, Y.C. Li, Z.G. Bi, J,H. Chen, *Langmuir*, 3 (2014) 900.
5. B. Xu, D.F. Zheng, M.Q. Jia, *Electrochimica Acta*, 16 (2013) 176.
6. C.L. Long, X. Chen, L.L. Jiang, *Nano Energy*, 12 (2015) 141.
7. S. Nagarajan, K. Subramani, M. Karnan, N. Ilayaraja, M. Sathish, *Energ. Fuel.*, 1 (2016) 71.
8. C. Long, L. Jiang, X. Wu, Y. Jiang, D .Yang, *Carbon*, 93 (2015) 412.
9. X. Wu, L. Jiang, C. Long, Z. Fan, *Nano Energy.*, 13 (2015) 527.
10. J. Li, J. Li, D. Yan, S. Hou, X. Xu, *J. Mater. Chem*., 6 (2018) 6595.
11. M. Xu, D. Li, Y. Yan, T. Guo, H. Pang, *Rsc Adv*. 69 (2017) 43780.
12. S. Sankar, H. wauk Lee, J. Hyun, A. Kim, AAA. Talha, *New J. Chem*., 22 (2017) 13792
13. M. Karnan, K. Subramani, N. Sudhan, N. Ilayaraja, M. Sathish, *Acs Appl. Mater. Interfaces*., 51 (2016) 35191.
14. W. Yang, W. Yang, L. Kong, A. Song, X. Qin, *Rsc Ad*., 87 (2017) 55257.
15. L. Zhang, L. Xu, Y. Zhang, X. Zhou, L. Zhang, *Rsc Adv*, 8 (2018) 3869.
16. Z. Dai, X. Shi, H. Liu, H. Li, Y. Han, *Rsc Adv.*,3 (2018) 1218.
17. W. Liu, Y. Yao, O. Fu, S. Jiang, Y. Fang, *Rsc Adv.*,7 (2017) 48537.
18. M. Klose, R. Reinhold, F. Logsch, F. Wolke, J. Linnemann, *Acs Sustain. Chem. Eng*., 5 (2017) 4094.
19. M. Ago, M. Borghei, J.S. Haataja, O.J. Rojas, *Rsc Adv.*, 89 (2016) 85802.
20. M. Biswal, A. Banerjee, M. Deo, S Ogale, *Energy Environ. Sci*., 4 (2013) 1249.
21. S. Hu, Y.L. Hsieh, *Rsc Adv*., 48 (2017) 30459.
22. X. Yang, M. Li, N. Guo, M. Yan, R. Yang, *Rsc Adv*., 6 (2016) 4365.
23. H. Peng, J. Zhou, K. Sun, G. Ma, Z. Zhang, *Acs Sustain. Chem. Eng*., 7 (2017) 5951.
24. Y.Q. Wang, B.S. Fugetsu, Z.P. Wang, W. Gong, I. Sakata, S. Morimoto, Y. Hashimoto, M. Endo, *Sci. Rep-UK*, 7 (2017) 40259.
25. T.N. Pham, T. Sharifi, R. Sandström, W. Siljebo, A. Shchukarev, K. Kordas, *Sci. Rep-UK*,1

(2017) 6112.
26. T. Purkait, G. Singh, D. Kumar, M. Singh, R.S. Dey, *Sci. Rep-UK*,1 (2018) 640.
27. X. Wu, Z. Tian, L. Hu, S. Huang, J. Cai, *Rsc Adv*., 52 (2017) 32795.
25. C. Zhang, Z. Pu, I.S. Amiinu, Y. Zhao, J. Zhu, *Nanoscale*., 10 (2018) 2902.
26. Y. Song, J. Liu, K. Sun, W. Xu, *Rsc Adv*., 76 (2017) 48324.
30. Z. Shen, H. Zhao, Y. Liu, Z. Kan, P. Xing, *React. Chem. Eng*., 3 (2018) 34.
31. Y. Cui, H. Wang, X. Xu, Y. Lv, J. Shi, *Sustain. Energ. Fuels*., 2 (2017) 381.
32. M. Hu, H. Zhou, X. Gan, L. Yang, Z.H. Huang, *J. Mater. Chem*., 4 (2017) 1582.
33. M. Serwar, U.A. Rana, H.M. Siddiqi, U.D. Khan, FAA. Ali, *Rsc Adv*., 86 (2017) 54626.
34. Y.L. Hu, X. Geng, L. Zhang, Z.M. Huang, J. Ge, Z.H. Li, *Sci. Rep-UK*, 1 (2017) 5849.
35. Q. Lv, W.Y. Si, J.J. He, L. Sun, C.F. Zhang, N. Wang, Z. Yang, X.D. Li, *Nat. Commun.* , 1 (2018) 3376.
33. D. Saha, Y.C. Li, Z.H. Bi, J.H. Chen, J.K. Keum, D. K. Hensley, *Langmuir*, 3(2014) 900.
37. Y.N. Gong, D. Lia, C.Z. Luo, Q. Fu, C.X. Pan, *Green. Chem.*, 17(2017) 19.
35. P. Dulyaseree, M. Fujishige, I. Yoshida, Y. Toya, Y. Banba, Y. Tanaka, T. Aoyama, M. Phonyiem, *Rsc Adv.*, 67(2017) 42064.
36 M. Ago, M. Borghei, J. S. Haatajab, O. J. Rojas, *Rsc Adv.*, 89(2016) 6
40. C. Wang, F.X. Wang, Z.C. Liu, Y.J. Zhao, Y. Liu, Q. Yue, H.W. Zhu, Y.H. Deng, *Nano Energy*, 41(2017) 674.